# Intramolecular Effects in Cellulose Mixed Benzyl Ethers Blended with Poly(ϵ-caprolactone)

CHARLES E. FRAZIER* and WOLFGANG G. GLASSER

Department of Wood Science and Forest Products, and Biobased Materials Center, Virginia Polytechnic Institute and State University, Blacksburg, Virginia 24061-0503

SYNOPSIS

Tri-*O*-benzyl cellulose, tri-*O*-*p*-fluorobenzyl cellulose, and a corresponding series of cellulose mixed benzyl ethers were synthesized and blended with poly(ϵ-caprolactone) (PCL). Mechanical and thermal analyses indicated that none of the cellulose benzyl ethers or the cellulose mixed benzyl ethers was miscible with PCL. However, there was evidence of a limited degree of compatibility that exhibited a dependence on the substituent ratio, or copolymer composition, of the cellulose mixed benzyl ethers. The weak interactions in these blends were found to be nonspecific, and thus the limited compatibility is thought to arise from intramolecular interactions within the cellulose mixed benzyl ethers. The treatment of cellulose mixed derivatives as copolymers and the potential use of intramolecular effects in cellulose derivative blending is discussed. © 1995 John Wiley & Sons, Inc.

## INTRODUCTION

As more and more research has been directed toward polymer blending, our understanding of polymer mixing and our ability to tailor blended materials have steadily improved. In the beginning there was little hope of finding many polymers whose solubility parameters were sufficiently similar to allow mixing in the limit of high molecular weight. The outlook brightened rapidly, however, when attention was directed toward promoting specific enthalpic interactions between polymer pairs. A somewhat recent discovery has provided another method of engineering miscible polymer blends in the absence of specific intermolecular interactions. This is in reference to miscibility windows between polymer pairs where at least one of the polymers is a copolymer. For example, consider monomer units 1, 2, and 3 where no specific interactions are possible. The monomers are sufficiently different in polarity that none of the respective homopolymers is miscible with the other. However, a copolymer made of units 1 and 2 is miscible with homopolymer 3, and the miscibility is restricted to a window defined by the copolymer composition. This window of miscibility arises from a large intramolecular mismatch in energy density between comonomer units 1 and 2. Or in terms of the binary interaction parameter $B$[1]:

$$B = B_{13}\phi_1 + B_{23}\phi_2 - B_{12}\phi_1\phi_2 \qquad (1)$$

where $B_{ij}$ is the interaction energy density between homopolymers $i$ and $j$ and $\phi_i$ is the volume fraction of $i$ in the copolymer. A negative $B$ is indicative of exothermic mixing; athermal mixing has a positive $B$. When a miscibility window arises without specific interactions, all $B_{ij}$ are positive, however, the intramolecular parameter, $B_{12}$, is a large positive such that the overall interaction parameter is negative and mixing for the system is exothermic. Some well-documented examples of this phenomenon are blends of poly(styrene-*co*-acrylonitrile) (SAN) with poly(ϵ-caprolactone)[2,3] as well as SAN blended with poly(methyl methacrylate).[4] The large positive intramolecular interaction has been referred to as an intramolecular "repulsive" effect.[5,6] In response, Krause[7] has reminded us that all interactions, however weak, are attractive in nature and that miscibility in these copolymer blends results not from repulsion but rather from the free energy minimi-

* To whom correspondence should be addressed.

Journal of Applied Polymer Science, Vol. 58, 1063–1075 (1995)
 CCC 0021-8995/95/061063-13

zation that is available to the system as a result of mixing. The utility of this phenomenon for engineering miscible blends is further demonstrated by Nishimoto et al.[4] They show how the binary interaction model is generally adequate for predicting miscibility in blends where at least one component is a copolymer or terpolymer.

These findings are pertinent to our own work in the polymer blending of cellulose mixed derivatives. Recall that cellulose is a linear polysaccharide composed of $\beta$-1,4-linked anhydroglucose units. The extent of cellulose derivatization is described by the degree of substitution ($DS$), which varies from 0 to 3 with respect to the three hydroxyls per anhydroglucose unit. Differential reactivity of the hydroxyl groups at positions 2, 3, and 6 gives rise to a heterogeneous substitution pattern along the length of the chain. Consequently, the resulting $DS$ is an average value taken over a possible eight different monomer units. The practical result is that all cellulosic polymers with a $DS$ between 0 and 3 are copolymeric in nature. This is not to say that any cellulose mixed derivative will be a random copolymer of eight different monomer units. On the contrary, the differential reactivity of the hydroxyls will likely promote a relative preponderance of any one repeat unit, with a few other repeat units present to a lesser degree.

Given this scenario, we can see that the thermodynamics of cellulose derivative blending could be strongly influenced by intramolecular effects. However, these effects would be difficult to observe in a polymer such as cellulose diacetate, for example. This is due to the likelihood that some of the intramolecular interaction parameters will be strongly negative as a result of hydrogen bonding between hydroxyl groups of dissimilar monomer units. This would contribute to an overall interaction parameter which is positive in magnitude, thus serving as a barrier to polymer mixing. The clear observation of intramolecular effects in cellulose derivative blending will have at least three requirements. Obviously, the first requirement is that the cellulose derivative must be a copolymer. In other words, it must be a mixed derivative, such as cellulose acetate butyrate (CAB). Second, the cellulose chain must be completely derivatized with no free hydroxyl groups that could promote specific intra- or intermolecular interactions. Finally, a blend system must be identified such that these effects may be observed. Using the example of CAB, we must find a polymer that is immiscible both with cellulose triacetate and cellulose tributyrate, but that is miscible with CAB as a function of the A/B ratio. This third requirement is the largest impediment to the observation of intramolecular effects in cellulose derivative blending. We can expect that time will reveal an appropriate system. Nevertheless, evidence of intramolecular effects is observable in immiscible systems that display a limited degree of compatibility or mechanical compatibility.

In the following discussion, the term "miscible" is reserved for those blends that display a negative free energy of mixing which is stable, thus forming a homogeneous phase on a molecular level. For the sake of clarity herein, a polymer blend is considered as either miscible or immiscible. This is not to say that intermediate degrees of mixing do not occur. For such cases and for present purposes, we define "compatibility" as an immiscible system which displays a limited degree of molecular mixing at phase boundaries such that physical properties of the blends are conserved or slightly enhanced. This has been referred to previously as mechanical compatibility.[8] Given these precepts, one can appreciate that molecular interactions may be discernible in miscible as well as immiscible systems. If molecular interactions are highly favorable, a negative free energy of mixing will promote a stable, homogeneous mixture, whereas an immiscible but mechanically compatible blend may display limited interactions at phase boundaries which are detectable with various analytical methods.

We report here on evidence for intramolecular effects in cellulose mixed benzyl ethers blended with PCL. A series of cellulose benzyl, *p*-fluorobenzyl mixed triethers which cover the spectrum of benzyl to *para*-fluorobenzyl ratios was synthesized. All cellulose tribenzyl ethers, regardless of composition, were found to be immiscible with PCL. However, some differential compatibility was found between PCL and these mixed benzyl ethers which appears as a function of the composition of the cellulose mixed benzyl ether.

## EXPERIMENTAL

### Materials

All solvents were freshly distilled with the appropriate desiccants prior to use. Unless otherwise stated, all reagents were purchased from Aldrich Chemical and used as received. Whatman cellulose type CF-11 was used as starting material in all cellulose reactions. The molecular weight of the starting cellulose was determined using the procedure of Evans and Wallace[9] in which the cellulose triphen-

ylurethane was synthesized and subsequently analyzed by GPC in THF. This cellulose had a $DP_n$ of 167 and a polydispersity of 1.67. The PCL used in this work was Tone 700, supplied by Union Carbide, with an $M_n$ of 30,000 g/mol, and a polydispersity of 1.7.

## Methods

### *Synthesis of Cellulose Tri-O-Benzyl Ethers and Cellulose Mixed Tri-O-Benzyl Ethers*

Tri-*O*-benzyl cellulose and tri-*O*-*p*-fluorobenzyl cellulose were synthesized using the appropriate chlorobenzylating reagent, starting with 10 g of cellulose according to the method described by Isogai et al.,[10] with the following exceptions. All reactions were carried out under nitrogen atmosphere. During the initial addition of benzylating reagent, the reaction was cooled in a water bath so as to counter the mixing exotherm. After the first addition of benzylating reagent, the flask was warmed to 70°C. Then there were 3 more additions of benzylating agent as per the method of Isogai et al.,[10] except these were at 1, 2, and 18 h after reaching 70°C. After the last addition of benzylating reagent, the reaction was heated to 85°C for 2 h. The flask was allowed to cool to room temperature, and the solution was poured into 4 L of distilled water. The polymer formed an emulsion which settled to the bottom of the beaker. The liquid layer was decanted off, and more distilled water was added with vigorous stirring. This procedure was repeated until the aqueous layer was colorless. Then the water was decanted off again, and 3 L of methanol was added to cause precipitation of the polymer. The product was filtered and extracted with methanol in a soxhlet for at least 24 h. The polymer was dried, dissolved in tetrahydrofuran, and centrifuged. The supernatant was concentrated and then precipitated into methanol. The polymer was finally dried at 50°C under 20 mm Hg vacuum for 24 h. Yields were typically 70 to 80% of theoretical.

A series of 5 different mixed benzyl ethers were synthesized using the same procedure described above. Mixed ethers were synthesized using different mole ratios of *p*-fluorobenzyl chloride and benzyl chloride. The following 5 mol ratios were used, fluorobenzyl/benzyl chloride: 75/25, 50/50, 40/60, 25/75, and 15/85. *p*-Fluorobenzyl chloride and benzyl chloride were added sequentially to the reaction flask. *p*-Fluorobenzyl chloride was always added before benzyl chloride. For example, in the synthesis using a mole ratio of 75/25 fluorobenzyl chloride to benzyl chloride, the first 3 additions of benzylating agent were fluorobenzyl chloride. When all of the fluorobenzyl chloride was used, only then was the benzyl chloride added. Elemental analysis was performed on all samples by Galbraith Laboratories (Knoxville, TN).

### *Molecular Weight Analysis*

THF was pumped by a Waters 510 HPLC pump through a series of 3 Waters Ultrastyragel columns, with pore sizes of $10^3$, $10^4$, and $10^6$ Å. Detection was with a Waters 410 refractometer, in series with a Viskotek differential viscometer model 100. The columns were heated to 40°C in an Eldex column heater, and both detectors were also heated to 40°C. THF was freshly degassed, and stored under a helium atmosphere during use. Narrow polydispersity, polystyrene standards from Polymer Laboratories were used to establish a universal calibration.

### *Nuclear Magnetic Resonance Spectroscopy*

A Varian Unity-400 NMR spectrometer was used to collect $^1$H-, $^{19}$F-, and $^{13}$C-NMR spectra. Samples were prepared by dissolving the analyzed material in the appropriate deuterated solvents, using 5- or 10-mm Wilmad glass tubes. Where appropriate, the percent fluorine present in a sample was determined with $^{19}$F-NMR using an internal standard analysis. Percentages of fluorine were calculated based upon the $^{19}$F integrations, and the known masses of sample and standard. The internal standard was 3-trifluoromethyl acetophenone (chemical shift = −64.26 ppm, relative to trifluoroacetic acid at −77.05 ppm). The substituent ratio, benzyl/*p*-fluorobenzyl, was measured with a quantitative $^{13}$C solution NMR pulse using inverted gated decoupling, where decoupling occurs only during FID acquisition. Chromium acetylacetonate was added to the solutions to enhance carbon relaxation.

### *Blend Preparation*

Blends were prepared by dissolving a mixture of both polymers in THF. A total of 4 g was dissolved in 25 mL of THF, with magnetic stirring. Stirring was continued until all polymer had dissolved, and the solution appeared homogeneous. Then the solution was filtered through Whatman, type-1, filter paper, and 5 additional mL of THF was poured through the filter. The final solution was approximately 4 g of solids dissolved in 30 mL of THF. This solution was poured into a Teflon mold, which was placed in a desiccator with the lid situated with about a 10

mm opening. All blends were solid to the touch after 4 days in the desiccator. The samples were taken from the mold and then vacuum dried under 20 mm Hg at 55°C for 48 h. After drying, the films, with average thickness and diameter of 2 mm and 10 cm, were packaged in air tight plastic storage bags. All films were stored in a −70°C freezer until analyzed.

### *Thermal Analysis*

Thermal transitions of polymers were observed using differential scanning calorimetry (DSC) and dynamic mechanical analysis (DMA). A Perkin Elmer, DSC-4, equipped with the Thermal Analysis Data System, TADS, was used with the Perkin Elmer Intracooler. The DSC was calibrated with high purity indium. Thin films of 6 mg or less were sealed in the usual sample holder. Melting transitions in PCL were measured at the point where the last trace of crystallinity disappeared at the end of the transition. This technique of $T_m$ assignment was not complicated by baseline aberrations because all signals were quite strong and easily distinguished from the baseline. Studies of $T_m$ depression were performed subsequent to annealing in order to prevent any lamellar reorganization as discussed in Results and Discussion. PCL crystallinity in the blends was measured using the heat of fusion of the first scan of the blends, ratioed to the heat of fusion for the pure PCL crystal, 139.5 J/g.[11] Isothermal crystallization studies were performed by heating the samples to 100°C and holding for 15 min. They were subsequently cooled at 10°C/min to the crystallization temperature and held there from 30 min to 10.5 h. After annealing, the samples were rapidly cooled to 30°C and scanned at 10°C/min. DMA was performed using a Polymer Laboratories DMTA. Samples in the shape of small rectangular bars were cut from films. Analysis was in single cantilever bending, at a frequency of 3 Hz, and displacement setting of 4×. Samples were scanned from −100°C to about 55°C.

### *Tensile Testing*

Small dogbones were punched from the films and analyzed at room temperature in tension using a Polymer Laboratories Miniature Materials-Minimat tester. The dogbone samples were 38 mm in length and the widths of the wide and narrow sections were 16 and 4.8 mm, respectively. All samples were deformed at a rate of 0.25 mm/min. Each data point is an average of 6–9 separate tests.

## RESULTS AND DISCUSSION

Recent work in our laboratory has dealt with the derivatization of cellulose in homogeneous solutions using solvent systems such as DMAc/LiCl or DMSO/$SO_2$/diethylamine (DEA). Using a modified version of the procedure of Isogai et al.,[10] cellulose benzylations were performed in DMSO/$SO_2$/DEA with excess powdered NaOH and the appropriate chlorobenzylating reagent. A total of seven cellulose benzyl ethers were synthesized, two homopolymers (tri-*O*-benzyl cellulose and tri-*O*-*p*-fluorobenzyl cellulose), and five mixed benzyl/*p*-fluorobenzyl triethers. Infrared analysis indicated that all cellulose derivatives were completely substituted. The degree of substitution of *p*-fluorobenzyl groups in the triethers is defined herein as the $DS_F$. Therefore, tri-*O*-benzyl cellulose has a $DS_F$ of 0; tri-*O*-*p*-fluorobenzyl cellulose has a $DS_F$ of 3, and the mixed ethers have a $DS_F$ between 0 and 3. All samples have an overall $DS$ of 3. $DS_F$ values were initially assigned using substituent ratios obtained from quantitative $^{13}$C-NMR. These numbers were subsequently verified with elemental analysis and also with an $^{19}$F internal standard NMR analysis. All $DS_F$ determinations agreed with each other within the limits of experimental error.

As reported elsewhere,[10] we also found that this benzylation reaction was extremely degradative to the cellulose $DP$. It was postulated that cellulose degradation was due to the combination of NaOH and atmospheric oxygen.[10] However, it was found that these reaction conditions were highly degradative to cellulose molecular weight when oxygen was excluded. In a separate study, DMSO/NaOH solutions (under $N_2$ gas) were slightly degradative to amylose, and the addition of $SO_2$ caused extensive depolymerization of amylose.[12] Consequently, it appears that NaOH coupled with the DMSO/$SO_2$/DEA solvent system is inherently degradative to the cellulose backbone, even in the absence of oxygen. Table I shows the molecular weight information for the seven cellulose derivatives synthesized. The $DP_n$ of the starting cellulose was 167. The sample with $DS_F$ equal to 2.9 stands out as having a molecular weight nearly double that of the other samples. The reason for this elevated molecular weight is unknown and may be due to some inadvertent variation in reaction conditions. The last column in Table I shows the Mark–Houwink–Sakurada (MHS) exponent obtained in THF at 40°C by differential viscometry. The MHS exponents indicate that all mixed benzyl ethers have similar solution conformations, while the two homopolymers define a range

**Table I Molecular Weight Information for Cellulose Benzyl, and Mixed Benzyl Ethers**

| | $M_n$ (grams/mole) | $DP_n$ | $DP_w$ | $\alpha^a$ |
|---|---|---|---|---|
| Tri-*O*-*p*-fluorobenzyl cellulose DSF 3.0 | 14,300 | 29 | 54 | 1.19 |
| Mixed cellulose tribenzyl ether DSF 2.9 | 27,300 | 56 | 119 | 0.96 |
| Mixed cellulose tribenzyl ether DSF 2.8 | 15,600 | 32 | 74 | 0.98 |
| Mixed cellulose tribenzyl ether DSF 2.0 | 18,500 | 40 | 87 | 1.0 |
| Mixed cellulose tribenzyl ether DSF 1.3 | 14,900 | 27 | 61 | 1.0 |
| Mixed cellulose tribenzyl ether DSF 0.65 | 13,300 | 30 | 68 | 1.0 |
| Tri-*O*-benzyl cellulose DSF 0.0 | 13,200 | 31 | 95 | 0.67 |

[a] Mark-Houwink-Sakurada (MHS) exponential factor.

of chain extension, from semiflexible for tri-*O*-benzyl cellulose to rodlike for tri-*O*-*p*-fluorobenzyl cellulose. Interestingly, a small amount of fluorine appears to extend the chain as the sample with $DS_F$ of 0.65 is significantly more extended than tri-*O*-benzyl cellulose. Likewise, the minuscule amount of nonfluorinated benzyl substituents in $DS_F$ 2.9 appears to flexibilize the chain in comparison to tri-*O*-*p*-fluorobenzyl cellulose.

Subtle differences in substituent ratios are evident in the $^{19}F$- and $^{13}C$-NMR. Figure 1 shows the $^{19}F$-NMR of all fluorinated cellulose benzyl ethers. Samples with $DS_F$ of 3.0, 2.9, and 2.8 display three sharp resonances corresponding to positions 2, 3, and 6 of the cellulose anhydroglucose unit. (No attempt was made to establish exact assignments.) These same spectra also show two small, overlapping resonances to the left of the major peaks, which probably are the reducing and nonreducing endgroups of the chains. The least fluorinated sample, $DS_F$ 0.65, displays multiple broad and overlapping fluorine signals. Consequently, there are several different fluorine environments located on the chain, which is evidence for a heterogeneous fluorine substitution pattern. This serves to emphasize the potential complexity of the copolymer composition for mixed cellulose derivatives. Among samples with a $DS_F$ of 3.0, 2.9, and 2.8, notice that the middle resonance in sample $DS_F$ 2.9 has a markedly reduced intensity relative to the other two major signals. This may be an indication of a relatively homogeneous substitution pattern of nonfluorinated benzyl groups in this sample. Besides this observation, the $^{19}F$-NMR does not show any clear difference between samples with $DS_F$ of 3, 2.9, and 2.8, however, the $^{13}C$-NMR does reveal fine differences. The $^{13}C$-NMR of samples with $DS_F$ of 2.0, 2.8, and 2.9 are displayed in Figure 2. The two signals centered at about 138.5

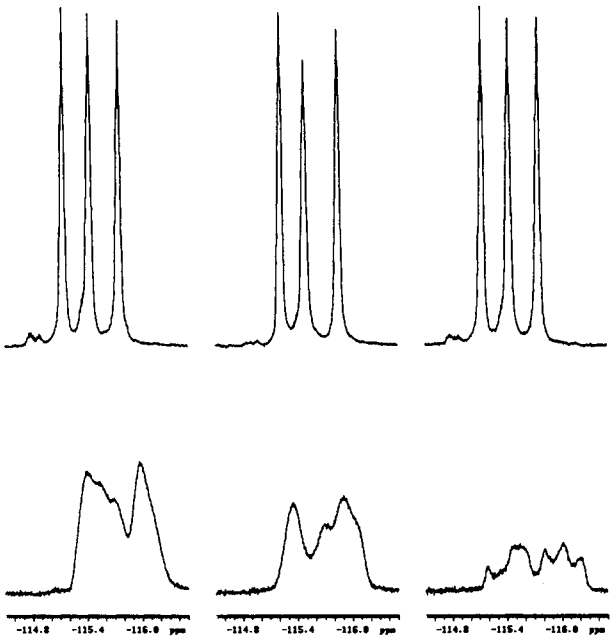


**Figure 1** $^{19}F$ solution NMR spectra of fluorinated cellulose benzyl ethers. In the top row from left, the samples are $DS_F$ 3, 2.9, and 2.8. In the bottom row from left, the samples are $DS_F$ 2.0, 1.3, and 0.65. Solvent is $CDCl_3$ and chemical shift reference is trifluoroacetic acid-$d_1$ at −77.05 ppm.

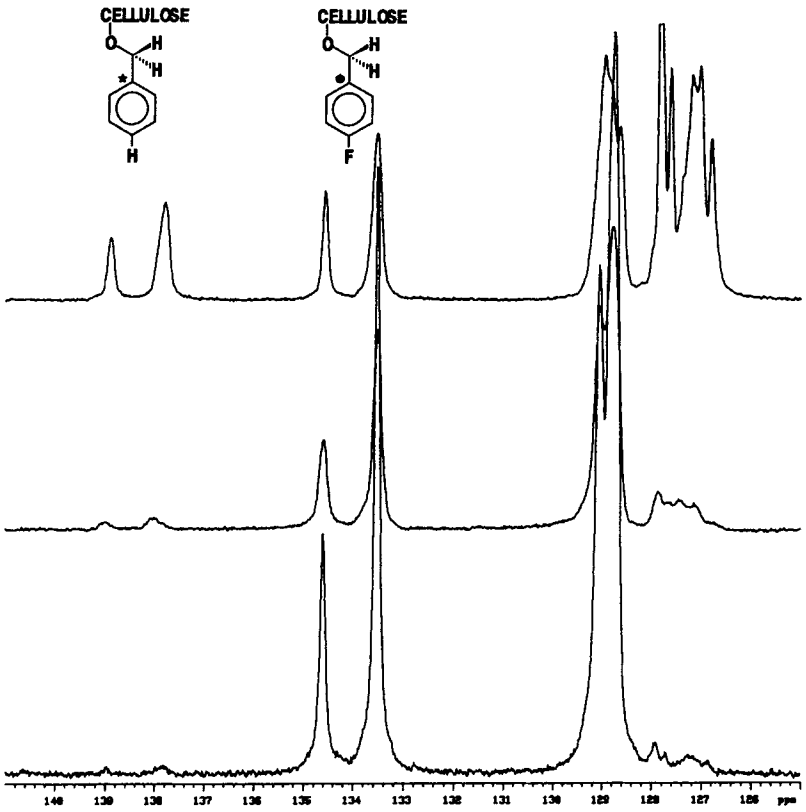


**Figure 2** $^{13}C$ solution NMR spectra of samples with $DS_F$ 2.0 (top), 2.8, and 2.9 (bottom). The two signals centered at 138.5 ppm are aromatic C1 carbons of nonfluorinated benzyl substituents. Signals centered at 134 ppm are aromatic C1 carbons of fluorobenzyl substituents. Solvent is $CDCl_3$.

ppm are carbons at the one position in the aromatic ring of nonfluorinated benzyl substituents. (These two peaks correspond to substituents at cellulose position 6, with substituents at cellulose positions 2 and 3 overlapping.) The same peaks for the fluorinated benzyl substituents are centered at about 134 ppm. Figure 2 shows that as the $DS_F$ rises from 2.0 to 2.9, the intensity of the signals centered at 134 ppm (fluorobenzyl C1) rises while the intensity of the signals centered at 138.5 ppm (benzyl C1) falls. Figure 2 also demonstrates a clear difference between samples of $DS_F$ 2.8 and 2.9, and it indicates that the $DS_F$ 2.9 sample is indeed a mixed benzyl ether with a very low amount of nonfluorinated benzyl substituents.

The thermal analysis of all of the cellulose benzyl ethers made in this study can be described as disappointing. None of the samples displayed a clear melting transition. Instead they typically showed a strong exotherm just prior to the onset of melting, which was always coincident with thermal decomposition (Fig. 3). (While thermogravimetric analysis was not performed, thermal degradation was evident from the sample discoloration seen in the sample after only one scan. Furthermore, subsequent scans of these samples produced only eratic noise in the

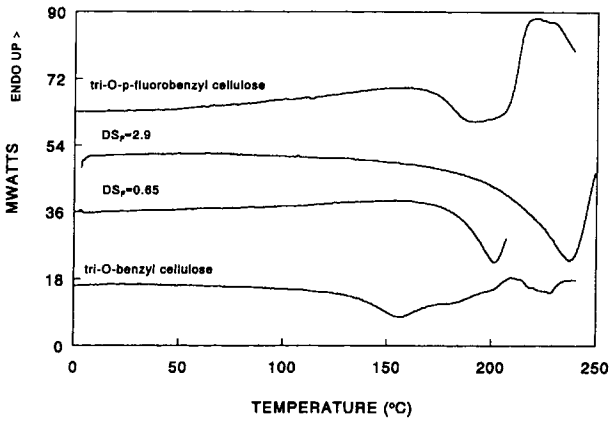


**Figure 3** DSC thermograms for selected cellulose benzyl ethers, showing first scans at a heating rate of 10°C/min. These samples were scanned in the form of powders which had been precipitated from THF and vacuum dried all under similar conditions.

region from 150 to 200°C.) This is in contrast to the clear melting endotherms occurring near 250°C shown for tri-*O*-benzyl cellulose by Isogai et al.[10] The only known difference between tri-*O*-benzyl celluloses in the respective works is that the molecular weights shown here are far less than in Isogai et al.[10] Glass transitions of the cellulose benzyl ethers were equally uneventful. All $T_g$s were very low in energy and thus required substantial effort to observe. For example, Figure 4 shows the glass transition of tri-*O*-*p*-fluorobenzyl cellulose and compares it to its $\alpha$-isomer, tri-*O*-*p*-fluorobenzyl amylose. The $T_g$s of all of the cellulose derivatives were similar to that shown in Figure 4, all in the range of 40 to 60°C. Furthermore, they could be observed only by thermally manipulating the samples, such as during a rapid heating preceded by slow cooling. These troublesome thermal properties meant that neither the $T_g$ nor the $T_m$ of the cellulose derivatives could be used as an indication of polymer mixing when blended with PCL. Furthermore, the low molecular weights of the cellulose derivatives made solution cast films of the pure cellulose derivatives too fragile to analyze by dynamic mechanical analysis. This problem also restricted us from making blends with more than 40% cellulose derivative, otherwise the mechanical integrity of the films suffered severely.

The final stage of blend preparation involved drying the films under vacuum at 55°C for 48 h. This relatively high drying temperature was selected in order to promote PCL crystal thickening, but not melting. The blends were white in color and not at all translucent, which is an indication that gross melting did not occur during drying. A few samples which did undergo melting were nearly transparent after drying and were excluded from this study. Our objective was to avoid the double endotherm which is often typical for the PCL melting transition.[13,14] The double endotherm has been attributed to melting–recrystallization–melting,[13] or to the possibility of two distinct lamellar thicknesses created during crystallization.[14] More recently, the double endotherm in poly(arylene-ether-ether-ketone) has been linked to the enthalpy relaxation of a rigid amorphous phase (low temperature endotherm) that forms only in the presence of the crystal phase (high temperature endotherm).[15] Whatever may be the origin of the double endotherm in PCL, its presence can potentially obscure crystallinity determinations using the DSC. As planned, first scans of all of the blends gave sharp and clear, single endothermic melting transitions, while subsequent scans generally resulted in double endotherms. During sample preparation, particular care was taken to ensure that all blends were dried at similar rates and to similar thicknesses. This is in response to the work of Runt and Rim who have shown that PCL crystallinity in blends is quite sensitive to the conditions of sample preparation.[16] The degree of PCL crystallinity in blends shown here is generally free from preparative effects. PCL blends with cellulose benzyl ethers of varying substituent ratios displayed only slight variation in PCL crystallinity. Figure 5 shows PCL crystallinity for two sets of THF cast blends; in this figure the substituent ratio has been converted to the percentage of fluorine in the cellulose derivative.

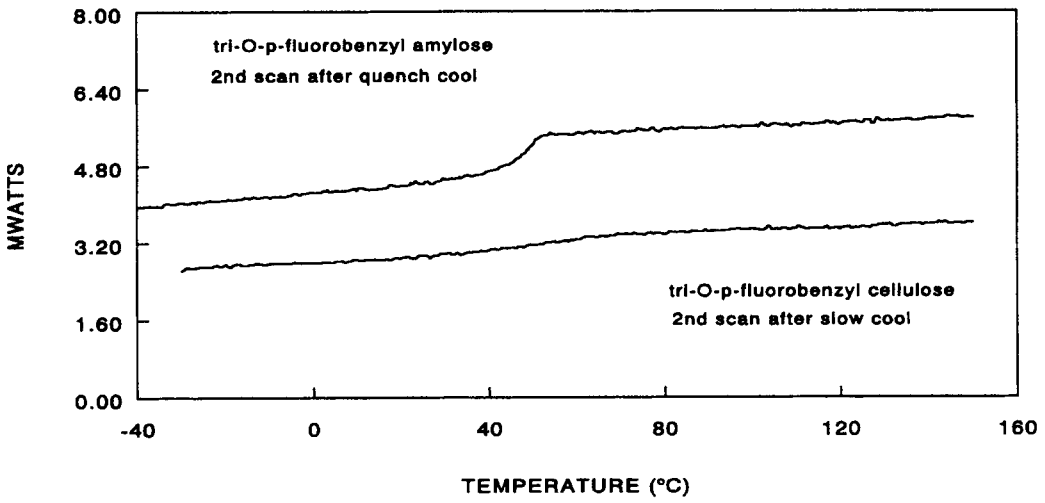


**Figure 4** DSC thermograms comparing tri-*O*-*p*-fluorobenzyl cellulose to tri-*O*-*p*-fluorobenzyl amylose. Heating rate for the cellulose derivative is 20°C/min and 10°C/min for the amylose derivative.

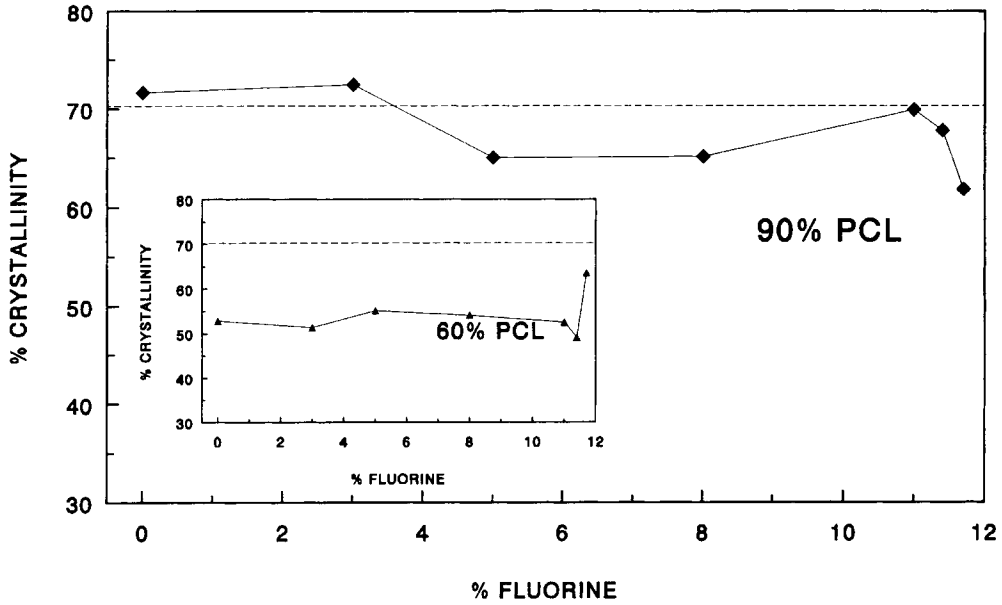


**Figure 5** Percentage PCL crystallinity in THF cast blends of cellulose benzyl ethers with PCL as a function of percentage fluorine in the cellulose derivative. The data are corrected for relative mass and the dotted line indicates the crystallinity of pure THF cast PCL. The composition of two series of blends are indicated by the %PCL.

The degree of mixing was first probed in blends with 90% PCL and 10% cellulose benzyl ether using simple tensile tests. PCL is a flexible chain polymer as indicated by its subambient $T_g$, and most cellulose derivatives are semiflexible to rodlike with $T_g$s often above ambient temperatures. Consequently, one should expect these cellulose benzyl ethers to enhance the physical properties of PCL blends if sufficient compatibility exists between the two polymers. The properties referred to here are Young's modulus, ultimate strain, and ultimate strength. Figures 6, 7, and 8 show the average tensile properties of these blends as a function of fluorine content in the cellulose derivative. The average moduli of all of the blends exceeds that of pure solvent cast PCL films. It also appears that the modulus tends toward higher values as the fluorine content of the cellulose benzyl ether rises. Curiously, the blend with 5% fluorine in the cellulose derivative ($DS_F$ = 1.3) has a remarkably higher modulus than any of the other samples. Furthermore, samples with the highest amounts of fluorine ($DS_F$ = 2.8, 2.9, and 3.0) show a slight downturn in modulus over a very nar-

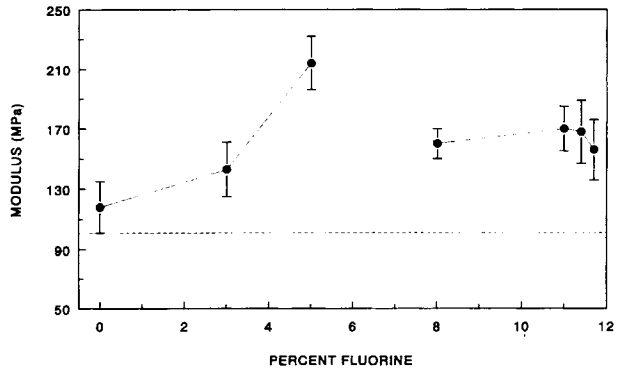


**Figure 6** Average modulus for a series of THF cast blends with 90% PCL and 10% cellulose benzyl ether, as a function of fluorine content of the cellulose derivative. The dotted line shows the average modulus of THF cast pure PCL.

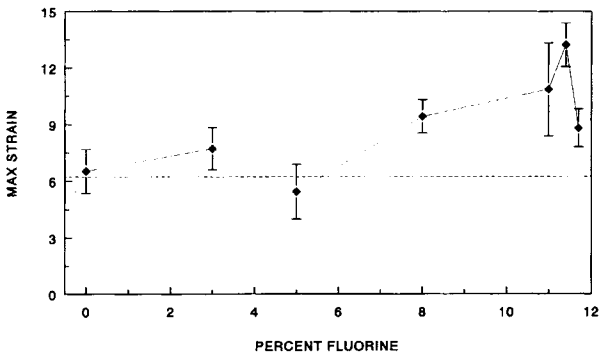


**Figure 7** Average maximum strain for a series of THF cast blends with 90% PCL and 10% cellulose benzyl ether, as a function of fluorine content of the cellulose derivative. The dotted line shows the average maximum strain of THF cast pure PCL.

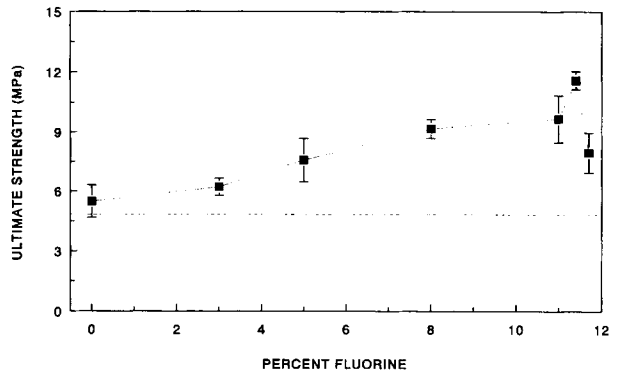


**Figure 8** Average ultimate strength for a series of THF cast blends with 90% PCL and 10% cellulose benzyl ether, as a function of fluorine content of the cellulose derivative. The dotted line shows the average ultimate strength of THF cast pure PCL.

row range of fluorine content. The moduli of all of the blends appear not to be significantly affected by the crystallinity of the PCL component; crystallinity is roughly constant according to Figure 5. The average maximum strain in these samples is very near that of pure PCL, until fluorine levels exceed 5% (Fig. 7). Above 5% fluorine, the average maximum strain rises until there is a discontinuity at the highest fluorine levels. Also, the average ultimate strength of the blends rises steadily until there is again a discontinuity at very high fluorine contents (Fig. 8). These tensile data indicate that fluorine promotes a degree of mechanical compatibility between cellulose benzyl ethers and PCL. Curiously, however, the best physical properties in these blends generally occur at fluorine levels slightly below the maximum. The blend with $DS_F$ 2.9 stands out among the blends with disproportionately high physical properties. This is probably due, in part, to the relatively high molecular weight of the $DS_F$ 2.9 sample as compared to the other cellulose benzyl ethers. Aside from possible molecular weight effects, the tensile data seem to indicate that the most favorable physical properties result from PCL blended with mixed benzyl ethers having a high fluorine content, or a high *p*-fluorobenzyl to benzyl substituent ratio.

After tensile tests, attention was turned to analysis of the PCL $T_g$ in these blends using dynamic mechanical analysis, DMA. DMA of pure PCL shows a maxima at about −40 to −45°C in the loss modulus, $E''$, and tan $\delta$, which is associated with the $T_g$.[17,18] For the sake of this discussion, we define the $T_g$ of these blends as the maxima in the loss modulus. Curves of tan $\delta$ are not shown here because they displayed no clear maxima, but instead they often showed only a continual rise in damping from −60

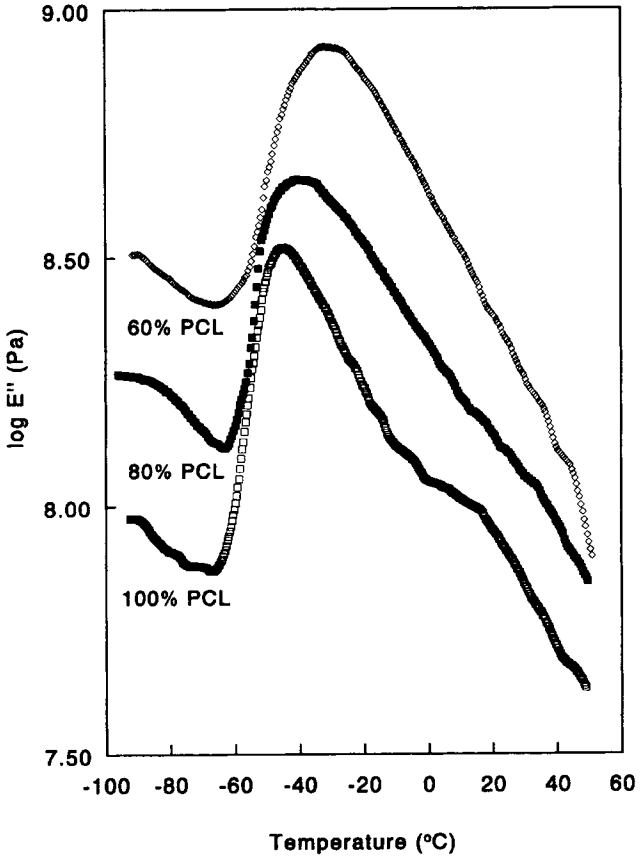


**Figure 9** Representative loss modulus curves for solvent cast blends of PCL with cellulose benzyl ether of $DS_F$ of 3.0. The top and bottom curves have been vertically shifted for clarity.

to 55°C, which made interpretation difficult. (This is suspected to have arisen from problems with sample clamping.) All of the $T_g$s reported hereafter are an average of 3 to 6 separate scans, except where noted otherwise.

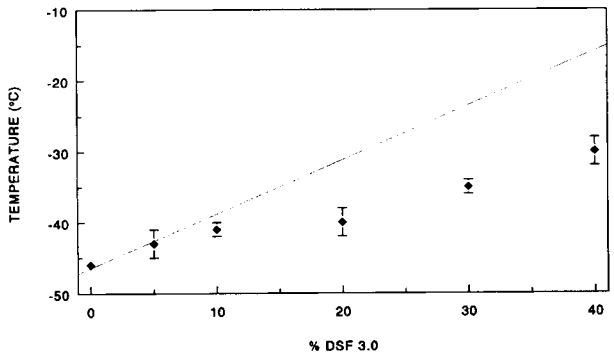


**Figure 10** Average $T_g$s as a function of blend composition for solvent cast blends of PCL with cellulose benzyl ether of $DS_F$ of 3.0. The solid line depicts the Fox relationship.

Another series of blends were prepared with PCL and tri-*O*-*p*-fluorobenzyl cellulose, $DS_F$ 3.0, spanning a range from 5 to 40% cellulose derivative. Figure 9 shows some representative loss modulus curves and Figure 10 shows the PCL $T_g$ as a function of blend composition. The maxima of the loss modulus rises slightly as the $DS_F$ 3.0 content increases, and the breadth of the transition widens considerably. With 40% of $DS_F$ 3.0, the PCL $T_g$ rises approximately 16°C, which is much less than would be expected from a weighted average of the respective transition temperatures. (The solid line in Figure 10 was calculated using a $T_g$ of 50°C for $DS_F$ 3.0, as taken from DSC.) These $T_g$ shifts indicate that some degree of interaction is occurring between PCL and tri-*O*-*p*-fluorobenzyl cellulose, but miscibility is not apparent. The addition of 40% $DS_F$ 3.0 caused a clear shift in the PCL $T_g$. Consequently, six additional blends were prepared with 60% PCL and 40% of each of the remaining cellulose benzyl and mixed benzyl ethers. The crystallinities of these solvent cast blends are shown in Figure 5, and the average $T_g$s from dynamic mechanical analysis are shown in Figure 11.

Surprisingly, Figure 11 shows that tri-*O*-benzyl cellulose, $DS_F = 0$, gives rise to the most significant PCL $T_g$ shift. This would indicate a higher level of compatibility than for any of the other fluorinated cellulose derivatives. This is in contrast to the tensile tests which indicated that the least amount of mechanical compatibility was occurring with the nonfluorinated cellulose benzyl ether. The tensile tests and dynamic mechanical analyses were with blends containing 10 and 40% cellulose derivative, respectively. It may be that the limited mechanical compatibility of the PCL/$DS_F = 0$ blend is compositionally dependent, which could explain the apparent contradiction. Besides this irregularity, the glass transitions of the remaining blends do not show a strong dependence on the cellulose derivative substituent ratio. It is noteworthy that the average $T_g$s of the blends display a discontinuity with cellulose derivatives of $DS_F$ equal to 2.8, 2.9, and 3.0. Recall that a similar situation arose from the tensile testing of the 90% PCL blends. However, the trends in Figure 11 may not be significant due to the narrow temperature range for the reported $T_g$s and also due to the relatively low number of samples scanned. We should further note that the $T_g$ of PCL is highly dependent upon sample crystallinity, where the transition temperature is raised by higher levels of crystallinity.[18] The crystallinities of the 60% PCL blends are roughly constant as a function of cellulose substituent ratio save the PCL blend with

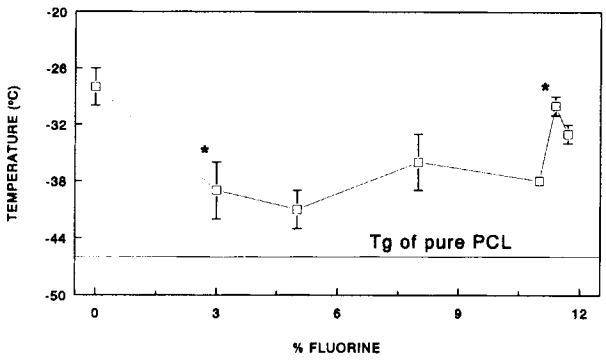


**Figure 11** Average $T_g$s from dynamic mechanical analysis of solvent cast blends of 60% PCL and 40% cellulose benzyl ether with variable fluorine content. All points are an average of three scans, except those points marked with an asterisk, which are an average of two scans.

$DS_F = 3.0$, which is approximately 20% higher in crystallinity.

The tensile properties and the glass transitions of these blends indicate a limited degree of interaction between PCL and cellulose benzyl ethers. Furthermore, the interaction displays a dependence upon the substituent ratio of the mixed benzyl ethers. The nature of this interaction was investigated by probing the blends with infrared spectroscopy. Thin films of the blends were cast from THF and analyzed at room temperature, and also in the melt at 65°C. The carbonyl signal of PCL was selected as an indicator of specific interaction. Specific interaction with the PCL carbonyl typically shifts the carbonyl signal to lower frequencies.[19,20] There was no indication of PCL carbonyl shift in the blends at room temperature or in the melt. Furthermore, the substituent ratio of the cellulose benzyl ethers had no observable effect on the PCL carbonyl signal. Hydrogen bonds or other dipole–dipole interactions with PCL must involve the carbonyl group of the polyester and should be observable in the infrared. As a result, we conclude that the limited interactions seen in these blends are nonspecific. Alternatively, it is possible that the interacting species are restricted to interfacial areas and are too few to detect.

This possibility was investigated with transmission electron microscopy, TEM. TEM of PCL blends with tri-*O*-benzyl cellulose and tri-*O*-*p*-fluorobenzyl cellulose indicated that the cellulose derivative is highly dispersed in the amorphous regions of PCL and that gross phase separation does not occur. Figure 12 shows the TEM micrograph of a blend of 10% $DS_F$ 3.0 blended with 90% PCL. In this particular micrograph, the sample is stained with ruthenium tetroxide, however, these blends appear the

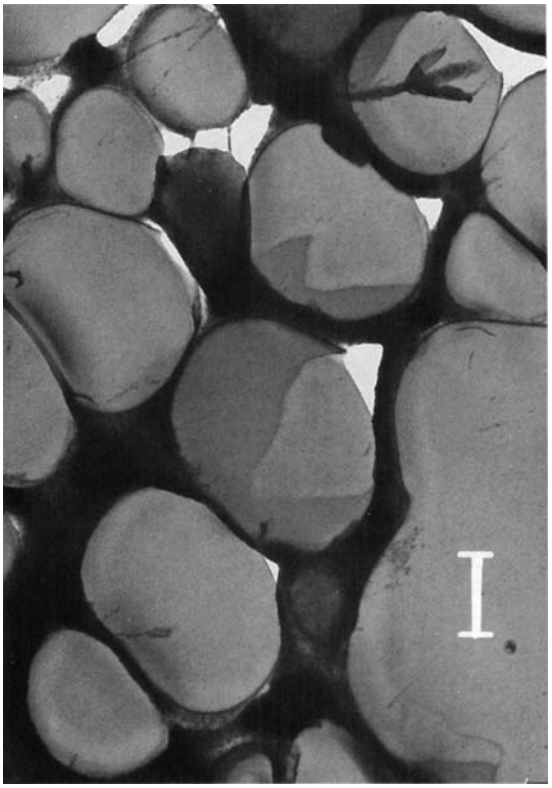

**Figure 12** Transmission electron micrograph of a THF cast blend of 90% PCL with 10% tri-*O*-*p*-fluorobenzyl cellulose. The bar equals 1.8 $\mu$m.

same with or without staining. The higher electron density of the cellulose derivative shows up as dark (black) regions. Figure 12 shows that the cellulose derivative is excluded from the light (gray) domains which are probably PCL spherulites. (The white regions are voids in the sample which resulted from preparation of the sample section.) The continuous matrix appears mostly black. However, careful inspection reveals a speckled appearance which corresponds to distinct domains of the cellulose derivative (on the order of tens of nanometers in diameter) dispersed within amorphous PCL. In light of the fine dispersion in the PCL amorphous regions, we should expect that specific molecular interactions would be detectable with infrared spectroscopy. Since this was not the case, we conclude that the limited interactions displayed in these blends are nonspecific.

As a final probe, we attempted to analyze PCL melting points under equilibrium conditions. However, difficulties were experienced in obtaining stable PCL crystals and so a complete Hoffman–Weeks analysis was not performed. It was found that PCL melting points and heats of fusion were stable when the samples were cooled from the melt and annealed at 55°C for at least 1 h. These isothermal crystallization conditions were applied to the same series of 60% PCL blends and no depression of the PCL melting point was found. In fact, all melting points were slightly elevated. Heats of fusion of isothermally crystallized blends were depressed with respect to pure PCL and were also variable as a function of the cellulose derivative substituent ratio (Fig. 13). Heats of fusion for the quench cooled samples also exhibited a dependence upon the cellulose derivative substituent ratio which was similar to the isothermally crystallized samples (Fig. 13). This information is similar to the above observations in that there appears to be a weak interaction between PCL and the cellulose benzyl ethers. These benzyl ethers have no real effect upon the melting temperature of PCL, but they do inhibit the crystallization of PCL under isothermal and quench cool conditions. Furthermore, the restraint of PCL crystallization, or the limited degree of interaction, appears as a function of the cellulose derivative substituent ratio. Also, we note again that a discontinuity appears across the three blends with cellulose derivatives of $DS_F$ equal to 2.8, 2.9, and 3.0.

The low molecular weights of the samples used in this study necessarily require some mention of the potential combinatorial contributions to the limited mixing seen in these blends. The $M_n$ of PCL is approximately 30,000 g/mol corresponding to a $DP_n$ of 263. The cellulose derivatives have $M_n$s ranging from 13,000 to 27,000 g/mol corresponding to $DP_n$s from about 30 to 50. Assuming a common segment reference volume of 100 cm$^3$/mol, combinatorial entropy driven miscibility ($X_{blend} < X_{crit}$) would require that the respective polymer solubility

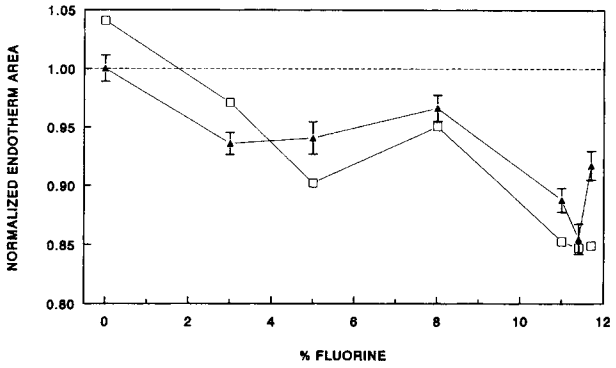


**Figure 13** Normalized melting endotherm areas for isothermally crystallized 60% PCL blends (open boxes) and also for quench cooled blends of the same composition (filled triangles). Each data point for the quench cooled samples is an average of 4 scans.

parameters differ by no more than about 0.42 (cal/cm$^3$)$^{1/2}$.[21] This would be a huge barrier to the athermal mixing of two high polymers with molecular weights in the millions. However, for the cases herein, combinatorial entropy could promote mixing due to the low molecular weights involved. The data in Figure 11 suggests that this is not the case. The $T_g$ shifts shown in Figure 11 are the greatest for films blended with samples of DSF equal to 2.9 and 0. These are, respectively, the samples with the greatest molecular weight and the broadest molecular weight distribution (Table I). If combinatorial effects were significant, one would expect these blends to exhibit the lowest $T_g$ shift under athermal mixing. The cellulose derivatives shown herein are generally similar in molecular weight and molecular weight distribution. If combinatorial effects were significant they would overwhelm the effects that the cellulose substituent ratio has on the limited mixing seen in these blends. In summary, the low molecular weights of these cellulose derivatives make combinatorial contributions to mixing a real possibility. However, the differential mixing (albeit limited) related to the substituent ratio of the mixed benzyl ethers suggests that combinatorial effects are not significant for these blends.

The above experiments indicate that a weak interaction occurs between PCL and cellulose tri-*O*-benzyl ether and tri-*O*-*p*-fluorobenzyl ether as well as the mixed benzyl/*p*-fluorobenzyl ethers. Evidence for the interaction is seen in (1) the enhanced physical properties of the blends as compared to pure PCL, (2) the small but significant increase of the PCL glass transition in the blends, (3) the good dispersion of cellulose benzyl ether in the amorphous phase of PCL as seen in TEM, and (4) the inhibition of PCL crystallization. It is also evident that this interaction is dependent upon the substituent ratio of the cellulose derivative. Generally, there appears to be an enhanced interaction between PCL and these cellulose benzyl ethers as the fluorine content of the derivatives rises. (One notable exception was seen in that the nonfluorinated sample produced the greatest $T_g$ shift according to dynamic mechanical analysis.) Most curious is the repeated discontinuity in properties among blends with $DS_F$ equal to 2.8, 2.9, and 3.0. This seems to indicate that the most favorable interaction occurs between PCL and cellulose derivatives with $DS_F$ equal to 2.8 and 2.9. Furthermore, it appears that the weak interactions shown here are nonspecific. These cellulose derivatives are completely substituted; therefore no hydrogen bonds will form between the respective polymers. On the other hand, it is conceivable that the carbon–fluorine dipole of the fluorobenzyl substituent may interact with the PCL carbonyl. For example, fluorobenzene groups are known for their susceptibility to ipso nucleophilic attack due to the large carbon–fluorine dipole. Such a dipole–dipole interaction would be expected to cause a shift in the carbonyl infrared absorption of PCL, but this was not observed. Furthermore, while there were small changes in the PCL $T_g$, and an apparent inhibition of crystallization, there was no reduction in PCL melting point in the blends. As stated, this points to the overall weakness of the interaction, which is counter to the effects expected from dipole–dipole interactions. Given that the interactions seen here are nonspecific, we must conclude that this blend system is affected by intramolecular effects arising from the copolymeric nature of the cellulose mixed benzyl ethers. With a possible eight different monomer units in the mixed benzyl ethers (MBE), we can see that the pairwise interaction model with PCL could become very complex, for example,

$$B_{\mathrm{PCL/MBE}} = \sum_{n=1}^{8} B_{n\mathrm{PCL}}\,\phi_n - (\tfrac{1}{2})\left[\sum_{n=1}^{8}\sum_{n'\neq n=1}^{8} B_{nn'}\phi_n\phi_{n'}\right] \quad (2)$$

In eq. (2), $n$ represents any one of the possible eight monomer units in the MBE, and $n'$ represents all monomer units in the mixed derivative different from $n$. The overall interaction parameter, $B_{\mathrm{PCL/MBE}}$, will be negative if one of the intramolecular interactions, let us say $B_{12}$, is a sufficiently large positive that it can overcome the intermolecular contributions. Any additional intramolecular contributions that would arise from a very complex copolymer would serve to dilute the effects of $B_{12}$ by a factor equal to the volume fraction of that additional pair. This was first discussed in Nishimoto et al.[4] On the other hand, other intramolecular interactions may also be highly positive and thus contribute to a negative overall interaction. Whatever the case may be, the potential complexity is self-evident. It is conceivable that the substitution pattern of a cellulose mixed derivative could be a smooth, or a discontinuous, function of the reagent feed ratio. The reaction conditions employed here appear to have created a discontinuous substitution pattern. Refer back to the $^{19}$F-NMR of Figure 1 and recall the difference in *p*-fluorobenzyl substitution pattern between samples with $DS_F$ equal to 2.8, 2.9, and 3.0. There is a noticeable difference in signal intensities be-

tween $DS_F$ 2.8 and 2.9, while samples $DS_F$ 3.0 and 2.8 are more similar. We do not claim a correlation between the substitution pattern shown in Figure 1 and the repeated discontinuity in properties shown for the corresponding blends. Rather we wish to emphasize the potential for manipulating blend miscibility by controlling the substitution pattern of cellulose mixed derivatives. We do believe that intramolecular effects are very likely responsible for the observations presented here. Unfortunately, none of the intramolecular pairwise interactions is sufficiently positive to drive miscibility with PCL.

It is remarkable that very slight differences in the cellulose derivative substituent ratio produce discernible differences in the compatibility with PCL. As mentioned, the intramolecular effects associated with blending mixed cellulose derivatives will be obvious only when a clear miscibility window is produced. We can be confident that such a system will eventually arise and thus open the door to a new method for engineering blends from cellulose derivatives.

## CONCLUSIONS

1. The $SO_2$/DEA/DMSO solvent system combined with NaOH is inherently degradative to the cellulose backbone, even in the absence of oxygen.
2. The *para*-fluorobenzyl substituent behaves as a cellulose backbone stiffener relative to the benzyl substituent.
3. PCL is immiscible with tri-*O*-benzyl cellulose, tri-*O*-*p*-fluorobenzyl cellulose, and the corresponding cellulose mixed benzyl ethers studied.
4. PCL does display a low degree of interaction with the above mentioned cellulose derivatives in the form of a limited compatibility, or mechanical compatibility.
5. The limited compatibility seen between PCL and these cellulose derivatives arises from nonspecific interactions which occur as a function of the substituent ratio, or copolymer composition.
6. In light of the absence of specific intermolecular interactions, the effect of copolymer composition on blend properties probably arises from intramolecular effects from within the cellulose mixed derivative. The future may prove that this phenomenon will be a valuable tool for engineering miscible blends with cellulose mixed derivatives.

We would like to acknowledge the financial support of the former Solar Research Institute, SERI, now known as the National Renewable Energy Laboratory, NREL. We would also like to thank Tom Glass in the Department of Chemistry at Virginia Tech for performing the quantitative $^{13}$C-NMR used in this work.

## REFERENCES

1. D. R. Paul and J. W. Barlow, *Polymer*, **25**, 487 (1984).
2. S. C. Chiu and T. G. Smith, *J. Appl. Polym. Sci.*, **29**, 1797 (1984).
3. V. Janarthanan, J. Kressler, F. E. Karasz, and W. J. Mcknight, *J. Polym. Sci.: Part B: Polym. Phys.*, **31**, 1013 (1993).
4. M. Nishimoto, H. Keskkula, and D. R. Paul, *Polymer*, **30**, 1279 (1989).
5. R. P. Kambour, J. T. Bendler, and R. C. Bopp, *Macromolecules*, **16**, 753 (1983).
6. J. L. G. Pfennig, H. Keskkula, J. W. Barlow, and D. R. Paul, *Macromolecules*, **18**, 1937 (1985).
7. S. Krause, *Macromolecules*, **24**, 2108 (1991).
8. J. V. Koleske, *Polymer Blends*, Vol. 2, 22, 369, D. R. Paul and S. Newman, Eds., New York, Academic Press, 1978.
9. R. Evans and A. F. A. Wallace, *Fourth Int. Symp. Wood Pulping Chem.*, **1**, 201 (1987).
10. A. Isogai, A. Ishizu, and J. Nakano, *J. Appl. Polym. Sci.*, **29**, 2097 (1984).
11. F. B. Khambatta, W. T. Russel, and R. S. Stein, *J. Polym. Sci., Polm. Phys. Ed.*, **14**, 1391 (1976).
12. C. E. Frazier, unpublished results.
13. P. B. Rim and J. P. Runt, *Macromolecules*, **16**, 762 (1983).
14. W. de Oliveira and W. G. Glasser, *Macromolecules*, **27**, 5 (1994).
15. V. Velikov and H. Marand, *Polym. Preprints*, **34**(2), 835 (1993).
16. J. Runt and P. B. Rim, *Macromolecules*, **15**, 1018 (1982).
17. C. J. Ong and F. P. Price, *J. Polym. Sci.: Polym. Symp.*, **63**, 45 (1978).
18. J. V. Koleske and R. D. Lundberg, *J. Polym. Sci., A-2*, **7**, 795 (1969).
19. M. M. Coleman and J. Zarian, *J. Polym. Sci.: Polym. Phys. Ed.*, **17**, 837 (1979).
20. D. F. Varnell, J. P. Runt, and M. M. Coleman, *Macromolecules*, **14**, 1350 (1981).
21. J. M. G. Cowie, *Macromol. Symp.*, **78**, 15 (1994).

*Received June 27, 1994*
*Accepted January 11, 1995*